Characterising the short-term habituation of event-related evoked potentials

Flavia Mancini[1, 2,*], Alessia Pepe[3], Giulia Di Stefano[3],
André Mouraux[4], Gian Domenico Iannetti[1]

[1]*Department of Neuroscience, Physiology and Pharmacology, University College London, London, UK*
[2]*Computational and Biological Learning Lab, Department of Engineering, University of Cambridge, Cambridge, UK*
[3]*Department of Neurological Sciences, University of Rome 'La Sapienza', Rome, IT*
[4]*Institute of Neuroscience, Université Catholique de Louvain, Brussels BE*

* *Corresponding author:*
Flavia Mancini
University of Cambridge
Department of Engineering, Computational and Biological Learning Lab
Trumpington Street, Cambridge, CB2 1PZ
fm456@cam.ac.uk

Abstract

Fast-rising sensory events evoke a series of functionally heterogeneous event-related potentials (ERPs). Stimulus repetition at 1 Hz is known to induce a strong habituation of the largest ERP responses, the vertex waves, which are elicited by stimuli regardless of their modality, provided that they are salient and behaviourally-relevant. In contrast, the effect of stimulus repetition on the earlier sensory components of ERPs has been less explored, and the few existing results are inconsistent. To characterize how the different ERP waves habituate over time, we recorded the responses elicited by 60 identical somatosensory stimuli (activating either non-nociceptive Aβ or nociceptive Aδ afferents), delivered at 1 Hz to healthy human participants. We show that the well-described spatiotemporal sequence of lateralised and vertex ERP components elicited by the first stimulus of the series is largely preserved in the smaller-amplitude, habituated response elicited by the last stimuli of the series. We also modelled the single-trial amplitude of both the somatosensory, lateralised wave (N1) and the supramodal centrally-distributed vertex waves (N2 and P2) elicited by the 60 stimuli. The vertex waves decayed monotonically, with a largest drop of response magnitude at the first stimulus repetition followed by much smaller decreases in subsequent repetitions. In contrast, the lateralised somatosensory waves did not habituate consistently across the block. Although the low signal-to-noise ratio of lateralised waves may have hindered our ability to detect consistent habituation effects, these results suggest a different degree of habituation of the different ERP components in response to stimulus repetition at 1 Hz.

Significance statement

Our results provide a functional characterization of the decay of the different ERP components when identical somatosensory stimuli are repeated at 1Hz. Fast-rising stimuli elicit ERPs obligatory contributed by both lateralised and vertex components, even when stimulus repetition minimizes stimulus relevance. The large vertex waves decay sharply at the first stimulus repetition, whereas smaller somatosensory, lateralised waves do not appear to habituate consistently across stimulus repetitions. Although the lack of consistent habituation of lateralised components may be contributed by the poor SNR of these small responses, it can also suggest that lateralised waves habituate either more slowly or to a less extent than vertex components of the ERP.

Introduction

Sudden sensory events evoke a series of transient responses in the ongoing electrocortical activity (event-related potentials, ERPs). ERPs are functionally heterogeneous and reflect the activity of distinct cortical generators overlapping in time and space (Sutton et al., 1965). Since these generators include both sensory and associative cortical areas, the scalp distribution of the ERPs elicited by stimuli of different modalities partly differs depending on the modality of the sensory input. In contrast, the scalp distribution of the largest ERP components is virtually identical regardless of the modality of the eliciting stimulus (Mouraux and Iannetti, 2009): it consists in a biphasic negative-positive deflection widespread over the scalp and maximal at the vertex – often referred to as 'vertex wave' or 'vertex potential' (Bancaud et al., 1953).

The vertex wave amplitude is maximal when fast-rising stimuli are presented using large and variable inter-stimulus intervals of several seconds (Mouraux and Iannetti, 2009; Huang et al., 2013), or when the stimulus reflects behaviourally relevant changes within a regular series of otherwise identical stimuli (Snyder and Hillyard, 1976; Valentini et al., 2011; Ronga et al., 2013). In contrast, when identical stimuli are monotonously repeated at short and regular intervals (e.g., 0.5 or 1 Hz), the vertex wave amplitude strongly decays (Jasper and Sharpless, 1956; Ritter et al., 1968; Davis et al., 1972; Mouraux and Iannetti, 2009; Liang et al., 2010; Wang et al., 2010). Although the decay of the vertex wave due to repeated stimulation at different stimulation frequencies has been described (Fruhstorfer et al., 1970; Greffrath et al., 2007), a formal characterization of how the different constituent components of the ERP habituate over time is still missing. This is particularly important considering that previous studies suggested that neural activity in different cortical regions may adapt to repeated stimulation at different timescales: for instance, neural activity in associative regions elicited by trains of innocuous, somatosensory stimuli decays faster than neural activity in sensory cortices (Forss et al., 2001; Venkatesan et al., 2014). However, these results may not generalise to responses elicited by noxious somatosensory stimuli: a previous study has suggested that the repetition of intra-epidermal nociceptive stimuli at 1 Hz for 1 minute suppresses evoked responses originating in primary somatosensory cortex (Mouraux et al., 2013).

Therefore, our primary objective was to describe the short-term habituation of the different constituents of somatosensory nociceptive and non-nociceptive ERPs: both the large centrally-distributed vertex waves and the smaller lateralised somatosensory waves. As in Mouraux et al. (2013), we recorded EEG while delivering trains of 60 identical stimuli at 1 Hz. In one group of healthy participants, we transcutaneously and electrically stimulated nerve trunks, activating directly all large-diameter Aβ somatosensory afferents and eliciting non-painful sensations. In a separate group of participants, we used radiant-heat stimuli that selectively activate skin nociceptors and elicit sensations of Aδ-mediated pinprick pain. We did not use intra-epidermal electrical stimulation of nociceptive afferents (Mouraux et al., 2013), because it can induce strong habituation of peripheral nociceptors (the stimulus is delivered always in the same location, whereas radiant heat stimuli can be easily displaced to reduce nociceptor fatigue). The use of two different somatosensory stimuli allowed to cross-validate and generalise our findings across different sensory pathways.

We addressed three complementary questions. (1) First, we asked whether the ERP amplitudes were different between the first and last stimuli of the block. (2) Second, we statistically assessed whether the

main response components were present in both the non-habituated ERP (i.e. the ERP elicited by the first stimulus of a series) and the habituated ERP (i.e. the ERP elicited by later stimuli that elicit a stable, habituated response). The rationale for this decision was the consistent observation that the amplitude of the main ERP waves (i.e., vertex waves) decays only minimally after the first few stimulus repetitions (Ritter et al., 1968; Fruhstorfer et al., 1969; Fruhstorfer et al., 1970; Fruhstorfer, 1971; Greffrath et al., 2007; Mouraux et al., 2013), a finding corroborated by the present results (Figures 1-4). (3) Third, we asked which decay functions best describe the habituation of different ERP components, by fitting a number of equations derived from previous studies (Fruhstorfer et al., 1970; Greffrath et al., 2007).

Methods

Participants

Thirty-two healthy subjects (14 women) aged 19–31 years (mean ± SD: 23.6 ± 3.9) participated in the study, after having given written informed consent. All experimental procedures were approved by the ethics committee of University College London (2492/001).

Transcutaneous electrical stimulation of Aβ fibers

Innocuous stimulation of Aβ afferents consisted of square-wave pulses (100 μs duration), generated by a constant current stimulator (DS7A, Digitimer, UK). Stimuli were delivered through a bipolar electrode placed above the superficial radial nerve, and elicited a paresthetic sensation in the corresponding innervation territory. Aβ detection thresholds were identified using the method of ascending staircases, on the right hand. The detection threshold was defined as the average of the lowest stimulus energy eliciting a sensation in 3 consecutive trials. Electrical stimuli were delivered at approximately 300% of each individual's Aβ detection threshold. Stimulus intensity was slightly adjusted to elicit sensations of comparable intensities on the left and right hands (mean ± SD, 17.4 ± 11.4 mA) and to make sure that the elicited sensation was never painful.

Cutaneous laser stimulation of Aδ and C fibers

Nociceptive stimuli were radiant heat pulses generated by an infrared neodymium:yttrium-aluminum-perovskite laser with a wavelength of 1.34 μm (Nd:YAP; Electronical Engineering, Italy). At this wavelength, laser pulses excite Aδ and C nociceptive free nerve endings in the epidermis directly and selectively, i.e. without coactivating touch-related Aβ fibers in the dermis (Bromm and Treede, 1984; Baumgartner et al., 2005; Mancini et al., 2014). The duration of each laser pulse was 4 ms.

Laser stimuli were delivered within a squared skin area (4 x 4 cm) centered on the dorsum of the hand, encompassing the area in which the stimulation of Aβ afferents elicited the paraesthesia. The laser beam was transmitted through an optic fiber, and its diameter at target site was set at ~6 mm by focusing lenses. A visible He–Ne laser pointed to the stimulated area, within which the laser beam was manually displaced after each stimulus. The laser was triggered by a computer script.

The method of ascending staircases used for identifying the detection threshold of Aβ stimuli was also used to identify the detection threshold of Aδ stimuli. For the EEG recordings, the stimulus energy was clearly above the activation threshold of Aδ fibers (0.53 ± 0.06 J/mm^2). This stimulus energy elicited intense but tolerable pinprick pain sensations, of comparable intensities on the right and left hands. Because variations in baseline skin temperature may modulate the intensity of the afferent nociceptive input (Iannetti et al., 2004), an infrared thermometer was used to ensure that the hand temperature varied no more than 1ºC across blocks. To avoid receptor fatigue or sensitization, the laser beam was displaced after each stimulus by ~1 cm within the predefined stimulated area.

Experimental procedure

Participants sat comfortably with their hands resting on a table in front of them. They were instructed to focus their attention on the stimuli, and fixate a yellow circular target (diameter: 1 cm) placed in front of them at a distance of approximately 60 cm from their face. A black curtain blocked the view of the hands. Throughout the experiment, white noise was played through headphones, to mask any sound associated with the either type of somatosensory stimulation.

The experiment was performed on 32 participants, divided in two groups of 16 participants. One group received electrical stimuli, and the other group received laser stimuli, using an identical procedure. Each participant received the somatosensory stimuli in 10 blocks, separated by a 5-minute interval, during which participants were allowed to rest. Each block consisted of 60 somatosensory stimuli delivered at 1 Hz: thus, each block lasted 1 minute. In each block, stimuli were delivered either to the right hand or to the left hand. Right- and left-hand blocks were alternated. The order of blocks was balanced across participants; half of the subjects started with a right-hand block, and the other half started with a left-hand block. At the end of each block, participants were asked to provide an average rating of perceived stimulus intensity, with reference to the modality of the stimulus and using a numerical scale ranging from 0 ("no shock sensation" or "no pinprick sensation") to 10 ("most intense shock sensation" or "most intense pinprick sensation"). This was done to ensure that the perceived intensity of the stimuli was similar across blocks (rating variability, SD across blocks: electrical stimuli, 0.2 ± 0.2; laser stimuli: 0.3 ± 0.4).

Electrophysiological recordings

EEG was recorded using 30 Ag–AgCl electrodes placed on the scalp according to the International 10-20 system (Electro-Cap International; USA), using the nose as reference. Electrode positions were 'Fp1', 'Fpz', 'Fp2', 'F7', 'F3', 'Fz', 'F4', 'F8', 'T3', 'C3', 'Cz', 'C4', 'T4', 'T5', 'P3', 'Pz', 'P4', 'T6', 'O1', 'Oz', 'O2', 'FCz', 'FC4', 'FC3', 'Cp3', 'Cp4'. Eye movements and blinks were recorded from the right *orbicularis oculi* muscle, using 2 surface electrodes. The active electrode was placed below the lower eyelid, and the reference electrode a few centimetres laterally to the outer canthus. Signals were amplified and digitized using a sampling rate of 1,024 Hz (SD32; Micromed, Italy).

EEG analysis

1. Preprocessing. EEG data were preprocessed and analyzed using Letswave 6 (http://www.nocions.org/letswave/) and EEGLAB (https://sccn.ucsd.edu/eeglab/). Continuous

EEG data were band-pass filtered from 0.5 to 30 Hz using a Butterworth filter, segmented into epochs using a time window ranging from -0.2 to 0.8 sec relative to the onset of each stimulus, and baseline corrected using the interval from -0.2 to 0 sec as reference. Trials contaminated by large artefacts (<10% in each block) were removed. Eye blinks and movements were corrected using a validated method based on unconstrained Independent Component Analysis ("runica" algorithm of EEGLAB). In all datasets, independent components related to eye movements showed a large EOG channel contribution and a frontal scalp distribution. To allow averaging across blocks while preserving the possibility of detecting lateralized EEG activity, scalp electrodes were flipped along the medio-lateral axis for all signals recorded in response to left hand stimulation.

2. Statistical assessment of ERP components. To assess decay of the ERP response, we first statistically compared the response amplitude at the beginning and at the end of the block (note that a more formal quantification of the response habituation was provided by the modelling analyses described in the next section). We performed four paired-sample t-tests to compare the amplitude of the response to the 1st stimulus vs the 2nd stimulus, and to the 1st vs the last (60th) stimulus. We also compared the amplitude of the ERPs elicited by the 2nd vs 3rd stimulus, and 59th vs 60th stimulus. All t-tests were performed for each time point of the ERP timecourse, and for all electrodes. Thus, this analysis yielded a scalp distribution of t-values across time, for each modality. To account for multiple comparisons, significant time points ($p < 0.05$) were clustered based on their temporal adjacency (cluster-level statistical analysis). For each cluster, we calculated the pseudo-*t* statistic of the two conditions, estimated its distribution by permutation testing (1000 times), and generated the bootstrap *p* values for testing the null hypothesis that there were no differences in signal amplitude (Maris and Oostenveld, 2007). This procedure identified the clusters in which the responses in two given conditions were significantly different.

Second, we assessed the consistency of stimulus-evoked modulations of EEG amplitude across time, to statistically evaluate whether EEG deflections in the post-stimulus time window (from 0 to +0.8 s) was significantly greater than baseline. Specifically, we performed a one-sample t-test against zero (i.e. against baseline) for each electrode and time point of the entire baseline-corrected waveform, using cluster-level permutation testing. This analysis yielded a scalp distribution of t-values across time, and was performed separately on the non-habituated ERP and on the habituated ERP of each modality. The non-habituated ERP was derived by averaging all the responses elicited by the 1st stimulus of all blocks. The habituated ERP was derived by averaging the responses elicited by the 6th to the 60th stimuli of all blocks. The decision of using these responses elicited by stimuli 6th to 60th as a proxy of the habituated ERP was based on the observation that the amplitude of the main ERP waves decays only minimally after the first 5 stimulus repetitions, as observed here (Figure 1-2, 4) and previously described (Fruhstorfer et al., 1970; Greffrath et al., 2007). Figures 1, 2, and 4 show how the amplitude of the ERPs was consistently habituated after the first few stimulus repetitions.

3. Modelling the within-block decay of the lateralised and vertex waves. We tested whether the amplitude of the N2 and P2 vertex waves and of the N1 lateralized wave evoked by Aβ and Aδ stimuli decayed following different functions derived from previous studies (Fruhstorfer et al., 1970; Greffrath et al., 2007). In each participant, we first averaged each of the 60 ERP responses across the 10 recording blocks, and thus obtained 60 average ERP waveforms: one for each of the 60 trials. Then, we averaged across participants and obtained 60 group-level averages. On these averages, we measured the latency and amplitude values of the 60 N2 and P2 peaks at Cz (referenced to the nose) and of the 60 N1 peaks

at Cc (referenced to Fz), using a validated procedure based on multiple linear regression (Hu et al., 2010; Hu et al., 2011). Finally, we modelled the decay of the N1, N2 and P2 peak amplitudes across the 60 trials, using three different equations:

(1) $y = a + \frac{b}{x}$

(2) $y = a + \frac{b}{x^c}$

(3) $y = a + b\, e^{-cx}$

where y is the peak amplitude of each given ERP wave, x is the trial number (from 1 to 60), e is the Euler constant, and a, b, c are the parameters to be estimated using a least squares method. Model fitting was performed on the signal averaged across subjects, rather than on each individual subject, because the signal-to-noise ratio of the habituated N1 wave is very low at single-trial and single-subject levels, making the extraction of N1 peaks not always reliable (Hu et al., 2010). We tested these specific models of ERP decay given the previous evidence that the vertex wave decays sharply at the first stimulus repetition (Fruhstorfer et al., 1970; Greffrath et al., 2007; Mouraux and Iannetti, 2009; Valentini et al., 2011; Ronga et al., 2013). No constraints were set on the parameters to be estimated. The decay of the N2 and P2 vertex components was modelled separately, because these waves can be independently modulated (Legrain et al., 2002; Hatem et al., 2007). To compare which model best fitted the data, we calculated the adjusted r^2 and the Akaike information criterion of each model, corrected for low sample size (AICc). The AIC is a relative estimate of the information lost in a given model, and it allows a fair comparison between non-linear models of different complexity, i.e. even when they have a different number of parameters. The lower the AIC, the better the model represents the measured data. From the difference in AICc values, we calculated the probability that each model was correct, with the probabilities summing to 100% (Burnham and Anderson, 2002). Finally, we tested for equal variance of the residuals using the 'test for appropriate weighting', as implemented in Prism GraphPad 7.0.

4. Code Accessibility. Modelling the within-block decay of the ERP waves was performed in Matlab 2016b. Data and code for fitting decay functions (equations 1-3) is openly accessible here: https://github.com/flamancini/ERP_habituation.git

Results

Response waveforms and topographies

Group-average ERPs elicited by Aβ and Aδ stimuli are shown in Figures 1, 2 and 3. As expected, the latency of Aδ-ERPs was longer than the latency of Aβ-ERPs, because Aδ fibers are thinly myelinated and thus have slower conduction velocity than large-myelinated Aβ fibers (Mountcastle, 2005).

Figure 1 shows that the amplitude decay of the negative and positive vertex waves (N2 and P2) elicited by the 60 repeated somatosensory stimuli. Both N2 and P2 dramatically decreased after the very first stimulus repetition (trial #1 vs. #2), in both stimulus modalities. In contrast, no wave except the Aβ-P2 further decreased at the second stimulus repetition (trial #2 vs. #3) (Figure 1). Figure 3 demonstrates

that, both in the non-habituated response (trial #1) and in the habituated response (average of trials #6-60), the N2 and P2 waves were greater than baseline. Not only they survived 1-minute of repeated stimulation, but clearly dominated the majority of the ERP responses.

Figure 2 shows the lack of any significant amplitude decay of the lateralized waves (N1 and P4) elicited by the 60 repeated somatosensory stimuli. In both stimulus modalities, these waves were much smaller than the vertex waves, as expected (Valentini et al., 2012; Hu et al., 2014). Paired t-tests showed no consistent habituation of the N1 and P4 waves at the first repetition of either Aβ or Aδ stimuli (trial #1 vs #2), and no significant habituation of any lateralised wave between the first and last stimulus of the block (trial #1 vs #60; Figure 2). Importantly, albeit small in amplitude, both the early N1 and the late P4 lateralized waves elicited in trials 1 and 6-60 were nevertheless consistently greater than baseline, as demonstrated by the point-by-point *t*-tests reported in Figure 3. The peaks of the N1 and P4 waves elicited in trials 1 and 6-60 had maximal spatial distribution over the central electrodes in the hemisphere contralateral to hand stimulation (Figure 3), as shown in previous studies (Hu et al., 2014; Mancini et al., 2015).

Modelling the decay of the vertex wave elicited by stimuli repeated at 1 Hz

Figure 4 displays the fit of the three models of ERP decay we tested on the average peaks of the N2, P2, and N1 waves. The same model best predicted the decay of the vertex N2 and P2 waves elicited by Aβ and Aδ stimuli. This winning model was equation #2, and the decay of the four peaks was described as follows:

$$\text{A}\beta\ \text{N2} = -4.22 - \frac{19.37}{x^{1.46}}$$

$$\text{A}\beta\ \text{P2} = 9.12 + \frac{14.52}{x^{1.35}}$$

$$\text{A}\delta\ \text{N2} = -5.01 - \frac{14.03}{x^{2.05}}$$

$$\text{A}\delta\ \text{P2} = 8.34 + \frac{14.37}{x^{2.51}}$$

where x is the trial number. The AICc and the adjusted r^2 values for all models are reported in Table I: the fitting of equation #2 gave the lowest AICc and the highest adjusted r^2 values. Furthermore, the residuals of the winning models were homoscedastic ($p > 0.999$). In qualitative terms, winning model #2 indicates that the amplitude of the examined peaks decays monotonically, with a fastest and sharpest drop of response magnitude at the first stimulus repetition, followed by much smaller decreases in the subsequent repetitions.

The fitting of the decay of the Aβ-N1 and Aδ-N1 waves was rather poor, possibly because of the low signal-to-noise ration at single-trial level. The winning model was again equation #2, although the coefficients of determination were low (adjusted $r^2 = 0.28$ for the Aβ-N1, and 0.33 for the Aδ-N1). This indicates that a large proportion of the variance of the data was not described by the winning model. Hence, none of the models that we chose *a priori* gave a sufficiently accurate description of the data. Therefore, we explored *post hoc* the fitting of other models (linear, power, sigmoidal, logistic, 1-6 degrees polynomial, and Fourier functions), but also these models poorly explained the variability of

Aβ-N1 and Aδ-N1 peak amplitude across stimulus repetitions (all adjusted $r^2 < \pm 0.1$). Thus, we found no consistent and reliable evidence of habituation of the N1 across the block.

Discussion

In this study, we characterised the habituation of the different components of the ERPs elicited by 60 identical somatosensory stimuli (activating either Aβ non-nociceptive, or Aδ nociceptive primary afferents) delivered at 1 Hz. Although the response amplitude was clearly reduced, the spatiotemporal sequence of the ERP waves was overall preserved in the habituated response (Figures 3). This was substantiated by point-by-point statistical analysis: both lateralised somatosensory components and vertex supramodal components typically observed in the ERP elicited by sporadic and unpredictable stimuli (Liang et al., 2010; Hu et al., 2014; Mancini et al., 2015) also contributed to the ERP elicited by frequent and predictable stimuli. Furthermore, our results indicate that the vertex components habituate dramatically at the very first stimulus repetition, whereas somatosensory, lateralised components do not decay consistently neither at the first stimulus repetition nor across 60 trials. We note, however, that lateralised components are small in amplitude, and their poor signal-to-noise ratio (SNR) is lower than vertex components – a factor that might have hindered our ability to detect a consistent habituation.

Effect of stimulus repetition on vertex ERP responses

The negative-positive vertex wave (VW) is the largest component of the EEG response elicited by sudden sensory stimuli. Its high signal-to-noise ratio makes the VW amplitude measurable in single trials, even when the response is habituated by stimulus repetition. Therefore, we were able to estimate the amplitude of the negative (N2) and positive (P2) vertex waves for each of the 60 ERPs (Figure 4). The decay of the negative and positive peaks was best modelled as follows:

$$y = a + \frac{b}{x^c}$$

where y is the peak amplitude of the N2 or P2 wave, x is the trial number, and a, b, c are the estimated parameters. This indicates that the amplitude of both vertex waves decays monotonically, with a largest, transient drop of response magnitude at the first stimulus repetition, followed by much smaller decreases in subsequent repetitions. This observation is further supported by point-by-point t-tests displayed in Figure 1.

Converging evidence indicates that stimuli of virtually all sensory modalities can elicit a VW, provided that they are salient enough (Liang et al., 2010). It is therefore not surprising that the VW elicited by auditory stimuli repeated at 1-Hz decays following a function similar to the one observed here for somatosensory stimuli (Fruhstorfer et al., 1970). Even when considering experimental observations that did not formally model the response habituation, the maximum decrease in VW amplitude consistently occurs at the first stimulus repetition, for auditory (Ritter et al., 1968; Fruhstorfer et al., 1970), somatosensory (Larsson, 1956; Fruhstorfer, 1971; Iannetti et al., 2008; Wang et al., 2010; Valentini et al., 2011; Ronga et al., 2013) and visual stimuli (Courchesne et al., 1975; Wastell and Kleinman, 1980). The similarity of the decay of the VW elicited by Aβ and Aδ stimuli (Figures 1, 3, 4) further supports the multimodal nature of the neural generators of these signals (Mouraux and Iannetti, 2009). The

365 mechanisms underlying such sharp reduction of response amplitude at the first stimulus repetition are
366 likely to be similar across sensory systems.
367
368 Before discussing the contribution of the present results in elucidating the functional significance of the
369 VW, it is important to highlight the empirical evidence that the observed response habituation is not
370 due to neural refractoriness of afferent neurons or to fatigue of primary receptors. A previous study
371 recorded ERPs elicited by pairs of nociceptive stimuli delivered at short intervals, which could be either
372 identical or variable across the block (Wang et al., 2010). Only when the inter-stimulus interval was
373 *constant* across the block, the VWs elicited by the second stimulus were reduced in amplitude. The peak
374 amplitude of the VWs elicited by the second stimulus was instead as large as the VWs elicited by the
375 first stimulus when the inter-stimulus interval was *variable*, indicating that neither neural refractoriness
376 nor fatigue can easily explain the sharp response decay to stimulus repetition.
377
378 Furthermore, if the sharp response habituation at the first stimulus repetition was determined by
379 fatigue of primary sensory receptors, we would have observed different decay profiles for stimuli
380 delivered in varying vs constant spatial locations. Indeed, the VW elicited by contact heat stimuli at long
381 and variable intervals (8-10 seconds) decays much faster if the second stimulus is delivered at the same
382 spatial location of the first (Greffrath et al., 2007). Instead, we observed remarkably similar patterns of
383 ERP decay for both Aδ laser stimuli delivered at different spatial locations and Aβ electrical stimuli
384 delivered in the same skin region. Additionally, electrical stimuli activate directly the axons in the nerve
385 trunk, bypassing the receptor, further ruling out receptor fatigue as explanation for the Aβ-ERP
386 habituation. Receptor fatigue might still contribute to the slow decrease in ERP magnitude observed
387 across dozens of stimulus repetitions of laser stimuli (Greffrath et al., 2007), but certainly not to the
388 dramatic reduction of ERP amplitude we observed after one single stimulus repetition.
389
390 The physiological significance of the VW remains to be properly understood. However, there is
391 evidence that this large electrocortical response reflects neural activities related to the detection of
392 salient environmental events (Jasper and Sharpless, 1956; Mouraux and Iannetti, 2009) and execution of
393 defensive movements (Moayedi et al., 2015). The detection of salient events relies on a hierarchical set
394 of rules that consider both their probability of occurrence and their defining basic features (Legrain et
395 al., 2002; Wang et al., 2010; Valentini et al., 2011; Ronga et al., 2013; Moayedi et al., 2016). The present
396 results are informative with respect to this functional framework. Indeed, stimulus repetition did not
397 abolish the VW elicited by either Aβ or Aδ stimuli, although it reduced its amplitude already after the
398 first stimulus repetition. Therefore, even when stimulus saliency is reduced by contextual factors, there
399 is a residual activity of the VW generators, only minimally reduced after the first few stimulus
400 repetitions (Figures 1, 3). These findings point towards the existence of an obligatory VW activity
401 triggered by any sudden and detectable change in the environment, even when contextual modulations
402 minimize its behavioural relevance.
403
404 Extensive evidence from cell physiology indicates that neural habituation to repeated stimuli arises
405 from alterations of synaptic excitability. Even the simple gill-withdrawal reflex in Aplysia dramatically
406 habituates at the first stimulus repetition (Byrne et al., 1978), due to a decreased drive from the sensory
407 neurons onto follower motor neurons (Castellucci et al., 1970; Carew and Kandel, 1973). The temporal
408 profile of this short-term habituation follows a fast decay function (Carew and Kandel, 1973), strikingly
409 similar to that observed in this and other studies on the habituation of electrocortical responses in

humans (Fruhstorfer et al., 1970; Greffrath et al., 2007). These synaptic changes have been interpreted as a hallmark of learning, and are central to the ability of the nervous system to adapt to environmental events (Carew and Kandel, 1973). Interpreting the decay of neural responses as functionally relevant for learning is not in contradiction with attentional interpretations: stimuli that are learned and recognized are likely to require less attentional resources than novel stimuli, and stimuli that need to be learned are typically more salient.

Effect of stimulus repetition on somatosensory lateralized responses

In somatosensory ERPs, the VW is both preceded and followed by other deflections of smaller amplitude. These have a topographical distribution maximal over centro-parietal electrodes in the hemisphere contralateral to hand stimulation. The earliest negative wave is usually referred to as N1 (Valentini et al., 2012) and the latest positive waveform of somatosensory ERPs is referred to as P4 (Hu et al., 2014; Mancini et al., 2015). Whereas the P4 has only been recently identified and its significance is not yet understood, the N1 has been described repeatedly in a large body of studies (Treede et al., 1988; Spiegel et al., 1996; Garcia-Larrea et al., 2003; Lee et al., 2009; Hu et al., 2014; Mancini et al., 2015), and largely reflect somatosensory neural activities (Lee et al., 2009; Liang et al., 2010). Both N1 and P4 are likely to originate in the primary somatosensory cortex (Treede et al., 1988; Valentini et al., 2012; Hu et al., 2014).

We showed that these somatosensory N1 and P4 responses are detectable not only in the response to the first stimulus, but also in the habituated ERP response, as supported by the statistical assessment of the scalp distribution of the ERP response elicited by both the first and the last stimuli of the series (Figure 3). This is important, given that a previous study using trains of intra-epidermal electrical shocks at 1 Hz failed to observe any lateralized response (Mouraux et al., 2013). We note, however, that in this previous study nociceptive afferents were activated using intra-epidermal electrical stimulation, which can cause strong peripheral and perceptual habituation, more significant than for radiant heat stimulation (Mouraux et al., 2010). Thus, in Mouraux et al (2013) peripheral habituation induced by repeated intra-epidermal electrical stimulation in the same skin location may have further reduced the already low SNR of N1 and P4 waves.

Although we clearly detected somatosensory lateralised waves elicited by trains of Aβ and Aδ stimuli at 1 Hz, we did not find strong evidence of any consistent effect of stimulus repetition on the amplitude of somatosensory, lateralised waves (Figures 2 and 4). As already noted, this might simply be due to the fact that N1 and P4 waves have small amplitudes and poor signal-to-noise ratio at single trial level (Hu et al., 2010). Nevertheless, a previous MEG study has also reported that neural activity originating from primary somatosensory cortex is more resilient to stimulus repetition (2-Hz pneumatic stimulation of the fingers and face): in other words, it decays to a less extent and more slowly than neural activity in higher-order cortical regions, such as the posterior parietal cortex (Venkatesan et al., 2014).

Our design was not suited to investigate the habituation of the earliest sensory components of SEPs, which typically require averaging responses elicited by hundreds of stimuli. However, we note that the N20 wave of SEPs, which originates in area 3b, is very resilient to stimulus repetition (Garcia Larrea et al., 1992) and is not modulated by selective spatial attention (Garcia-Larrea et al., 1991). In contrast, the later N1 waves of SEPs and LEPs can be modulated by spatial attention (Legrain et al., 2002), but perhaps to a less extent than the vertex waves.

In conclusion, our results provide a functional characterization of the decay of the different ERP components when identical somatosensory stimuli are repeated at 1Hz. Fast-rising stimuli elicit ERPs obligatory contributed by both lateralised and vertex components, even when stimulus repetition minimizes stimulus relevance. The large vertex waves decay sharply at the first stimulus repetition, whereas smaller somatosensory, lateralised waves do not appear to habituate consistently across stimulus repetitions. Although the lack of consistent habituation of lateralised components may be contributed by the poor SNR of these small responses, it can also suggest that lateralised waves habituate either more slowly or to a less extent than vertex components of the ERP.

Figure captions

Figure 1. *Habituation of vertex waves (N2, P2) elicited by repeated Aβ (left panel) and Aδ (right panel) stimuli.* The figure shows the ERPs elicited by 60 stimuli delivered at 1 Hz, at electrode Cz referenced to the nose (vertex waves). The responses to both the first five stimuli and the last five stimuli are enlarged and presented super-imposed, to facilitate visual comparison. To assess possible habituation effects, we used paired-sample *t*-tests with cluster-based permutation testing to compare the amplitude of the ERP elicited in trial #1 vs #2, trial #1 vs #60, trial #2 vs #3, and trial #59 vs #60, for each time point of the waveform and scalp electrode. Point-by-point *t* values are shown on the bottom panels of the figure. Time intervals during which the ERP waves were significantly different at $p < 0.05$ are highlighted in orange. The scalp distributions of *t* values are also displayed at the latencies of the maximum/minimum *t* values in the time-windows of the N2 and P2 waves, for the trial #1 vs #60 comparisons.

Figure 2. *Habituation of lateralized somatosensory waves (N1, P4) elicited by repeated Aβ (left panel) and Aδ (right panel) stimuli.* The figure shows the ERPs elicited by 60 stimuli delivered at 1 Hz, at electrode Cc referenced to Fz. The responses to both the first five stimuli and the last five stimuli are enlarged and presented super-imposed, to facilitate visual comparison. To assess possible habituation effects, we used paired-sample *t*-tests with cluster-based permutation testing to compare the amplitude of the ERP elicited in trial #1 vs #2, trial #1 vs #60, trial #2 vs #3, and trial #59 vs #60, for each time point of the waveform and scalp electrode. Point-by-point *t* values are shown on the bottom panels of the figure. Time intervals during which the ERP waves were significantly different at $p < 0.05$ are highlighted in orange.

Figure 3. *Habituation of vertex waves (N2, P2) and lateralized responses (N1, P4) elicited by Aβ (top panel) and Aδ (right panel) somatosensory stimuli.* Displayed signals show group-level ERPs recorded from the vertex (Cz vs nose) and from the central electrode contralateral to the stimulated hand (Cc vs Fz), elicited by the first stimulus in a series (non-habituated response) and by the average of trials #6-60 (habituated response). Scalp topographies (signals referenced to the nose) are displayed at the peak latency of the N1, N2, P2, and P4 waves, in all conditions. To assess the consistency of stimulus-evoked modulations of ERP amplitude across time, we performed a one-sample *t*-test against zero (i.e. against baseline) with cluster-based permutation testing, for each electrode and time point of the waveform. Point-by-point *t* values are shown below the ERPs. Time intervals during which the ERP waves were significantly different than 0 in the N1, N2, P2, and P4 time windows are highlighted in orange.

Figure 4. *Modelling the decay of the vertex waves (N2, P2) and lateralized waves (N1) elicited by repeated Aβ (left panels) and Aδ (right panels) stimuli.* The average peak amplitudes of the N2 (blue circles), P2 (yellow circles) and N1 waves (lilac circles) are displayed for each of the 60 trials. The function that best fit the decay of the N2 and P2 amplitudes (equation #2 in the main text, here indicated by the arrow) is displayed with a black dashed line.

Acknowledgments

FM and GDI were supported by a Wellcome Trust Strategic Award (COLL JLARAXR). GDI is additionally supported by a ERC Consolidator Grant (PAINSTRAT) and by the Medical Research Council. AM is supported by an ERC Starting Grant (PROBING-PAIN). The authors declare no competing financial interests.

References

Bancaud J, Bloch V, Paillard J (1953) [Encephalography; a study of the potentials evoked in man on the level with the vertex]. Rev Neurol (Paris) 89:399-418.

Baumgartner U, Cruccu G, Iannetti GD, Treede RD (2005) Laser guns and hot plates. Pain 116:1-3.

Bromm B, Treede RD (1984) Nerve fibre discharges, cerebral potentials and sensations induced by CO2 laser stimulation. Hum Neurobiol 3:33-40.

Burnham KP, Anderson DR (2002) Model Selection and Multimodel Inference, 2nd Edition: Springer-Verlag.

Byrne JH, Castellucci VF, Kandel ER (1978) Contribution of individual mechanoreceptor sensory neurons to defensive gill-withdrawal reflex in Aplysia. J Neurophysiol 41:418-431.

Carew TJ, Kandel ER (1973) Acquisition and retention of long-term habituation in Aplysia: correlation of behavioral and cellular processes. Science 182:1158-1160.

Castellucci V, Pinsker H, Kupfermann I, Kandel ER (1970) Neuronal mechanisms of habituation and dishabituation of the gill-withdrawal reflex in Aplysia. Science 167:1745-1748.

Courchesne E, Hillyard SA, Galambos R (1975) Stimulus novelty, task relevance and the visual evoked potential in man. Electroencephalogr Clin Neurophysiol 39:131-143.

Davis H, Osterhammel PA, Wier CC, Gjerdingen DB (1972) Slow vertex potentials: interactions among auditory, tactile, electric and visual stimuli. Electroencephalogr Clin Neurophysiol 33:537-545.

Forss N, Narici L, Hari R (2001) Sustained activation of the human SII cortices by stimulus trains. Neuroimage 13:497-501.

Fruhstorfer H (1971) Habituation and dishabituation of the human vertex response. Electroencephalogr Clin Neurophysiol 30:306-312.

Fruhstorfer H, Jarvilehto T, Soveri P (1969) Short-term habituation and dishabituation of the sensory evoked response in man. Acta Physiol Scand 76:14A-15A.

Fruhstorfer H, Soveri P, Jarvilehto T (1970) Short-term habituation of the auditory evoked response in man. Electroencephalogr Clin Neurophysiol 28:153-161.

Garcia Larrea L, Bastuji H, Mauguiere F (1992) Unmasking of cortical SEP components by changes in stimulus rate: a topographic study. Electroencephalogr Clin Neurophysiol 84:71-83.

Garcia-Larrea L, Bastuji H, Mauguiere F (1991) Mapping study of somatosensory evoked potentials during selective spatial attention. Electroencephalogr Clin Neurophysiol 80:201-214.

Garcia-Larrea L, Frot M, Valeriani M (2003) Brain generators of laser-evoked potentials: from dipoles to functional significance. Neurophysiol Clin 33:279-292.

Greffrath W, Baumgartner U, Treede RD (2007) Peripheral and central components of habituation of heat pain perception and evoked potentials in humans. Pain 132:301-311.

Hatem SM, Plaghki L, Mouraux A (2007) How response inhibition modulates nociceptive and non-nociceptive somatosensory brain-evoked potentials. Clin Neurophysiol 118:1503-1516.

Hu L, Mouraux A, Hu Y, Iannetti GD (2010) A novel approach for enhancing the signal-to-noise ratio and detecting automatically event-related potentials (ERPs) in single trials. NeuroImage 50:99-111.

Hu L, Valentini E, Zhang ZG, Liang M, Iannetti GD (2014) The primary somatosensory cortex contributes to the latest part of the cortical response elicited by nociceptive somatosensory stimuli in humans. NeuroImage 84:383-393.

Hu L, Liang M, Mouraux A, Wise RG, Hu Y, Iannetti GD (2011) Taking into account latency, amplitude, and morphology: improved estimation of single-trial ERPs by wavelet filtering and multiple linear regression. Journal of Neurophysiology 106:3216-3229.

Huang G, Xiao P, Hung YS, Iannetti GD, Zhang ZG, Hu L (2013) A novel approach to predict subjective pain perception from single-trial laser-evoked potentials. NeuroImage 81:283-293.

Iannetti GD, Hughes NP, Lee MC, Mouraux A (2008) Determinants of laser-evoked EEG responses: pain perception or stimulus saliency? J Neurophysiol 100:815-828.

Iannetti GD, Leandri M, Truini A, Zambreanu L, Cruccu G, Tracey I (2004) Adelta nociceptor response to laser stimuli: selective effect of stimulus duration on skin temperature, brain potentials and pain perception. Clin Neurophysiol 115:2629-2637.

Jasper H, Sharpless S (1956) Habituation of the arousal reaction. Brain 79:655-680.

Larsson LE (1956) The relation between the startle reaction and the non-specific EEG response to sudden stimuli with a discussion on the mechanism of arousal. Electroencephalogr Clin Neurophysiol 8:631-644.

Lee MC, Mouraux A, Iannetti GD (2009) Characterizing the cortical activity through which pain emerges from nociception. J Neurosci 29:7909-7916.

Legrain V, Guerit JM, Bruyer R, Plaghki L (2002) Attentional modulation of the nociceptive processing into the human brain: selective spatial attention, probability of stimulus occurrence, and target detection effects on laser evoked potentials. Pain 99:21-39.

Liang M, Mouraux A, Chan V, Blakemore C, Iannetti GD (2010) Functional characterisation of sensory ERPs using probabilistic ICA: effect of stimulus modality and stimulus location. Clin Neurophysiol 121:577-587.

Mancini F, Beaumont AL, Hu L, Haggard P, Iannetti GD (2015) Touch inhibits subcortical and cortical nociceptive responses. Pain 156:1936-1944.

Mancini F, Bauleo A, Cole J, Lui F, Porro CA, Haggard P, Iannetti GD (2014) Whole-body mapping of spatial acuity for pain and touch. Ann Neurol 75:917-924.

Maris E, Oostenveld R (2007) Nonparametric statistical testing of EEG- and MEG-data. J Neurosci Methods 164:177-190.

Moayedi M, Liang M, Sim AL, Hu L, Haggard P, Iannetti GD (2015) Laser-Evoked Vertex Potentials Predict Defensive Motor Actions. Cereb Cortex.

Moayedi M, Di Stefano G, Stubbs MT, Djeugam B, Liang M, Iannetti GD (2016) Nociceptive-Evoked Potentials Are Sensitive to Behaviorally Relevant Stimulus Displacements in Egocentric Coordinates. eNeuro 3.

Mountcastle VB (2005) Neural mechanisms of somatic sensation. Cambridge, Massachusetts: Harvard University press.

Mouraux A, Iannetti GD (2009) Nociceptive laser-evoked brain potentials do not reflect nociceptive-specific neural activity. J Neurophysiol 101:3258-3269.

Mouraux A, Iannetti GD, Plaghki L (2010) Low intensity intra-epidermal electrical stimulation can activate Adelta-nociceptors selectively. PAIN 150:199-207.

Mouraux A, De Paepe AL, Marot E, Plaghki L, Iannetti GD, Legrain V (2013) Unmasking the obligatory components of nociceptive event-related brain potentials. Journal of Neurophysiology 110:2312-2324.

Ritter W, Vaughan HG, Jr., Costa LD (1968) Orienting and habituation to auditory stimuli: a study of short term changes in average evoked responses. Electroencephalogr Clin Neurophysiol 25:550-556.

Ronga I, Valentini E, Mouraux A, Iannetti GD (2013) Novelty is not enough: laser-evoked potentials are determined by stimulus saliency, not absolute novelty. Journal of Neurophysiology 109:692-701.

Snyder E, Hillyard SA (1976) Long-latency evoked potentials to irrelevant, deviant stimuli. Behav Biol 16:319-331.

Spiegel J, Hansen C, Treede RD (1996) Laser-evoked potentials after painful hand and foot stimulation in humans: evidence for generation of the middle-latency component in the secondary somatosensory cortex. Neurosci Lett 216:179-182.

Sutton S, Braren M, Zubin J, John ER (1965) Evoked-potential correlates of stimulus uncertainty. Science 150:1187-1188.

Treede RD, Kief S, Holzer T, Bromm B (1988) Late somatosensory evoked cerebral potentials in response to cutaneous heat stimuli. Electroencephalogr Clin Neurophysiol 70:429-441.

Valentini E, Torta DM, Mouraux A, Iannetti GD (2011) Dishabituation of laser-evoked EEG responses: dissecting the effect of certain and uncertain changes in stimulus modality. J Cogn Neurosci 23:2822-2837.

Valentini E, Hu L, Chakrabarti B, Hu Y, Aglioti SM, Iannetti GD (2012) The primary somatosensory cortex largely contributes to the early part of the cortical response elicited by nociceptive stimuli. NeuroImage 59:1571-1581.

Venkatesan L, Barlow SM, Popescu M, Popescu A (2014) Integrated approach for studying adaptation mechanisms in the human somatosensory cortical network. Exp Brain Res 232:3545-3554.

Wang AL, Mouraux A, Liang M, Iannetti GD (2010) Stimulus novelty, and not neural refractoriness, explains the repetition suppression of laser-evoked potentials. Journal of Neurophysiology 104:2116-2124.

Wastell DG, Kleinman D (1980) Fast habituation of the late components of the visual evoked potential in man. Physiol Behav 25:93-97.

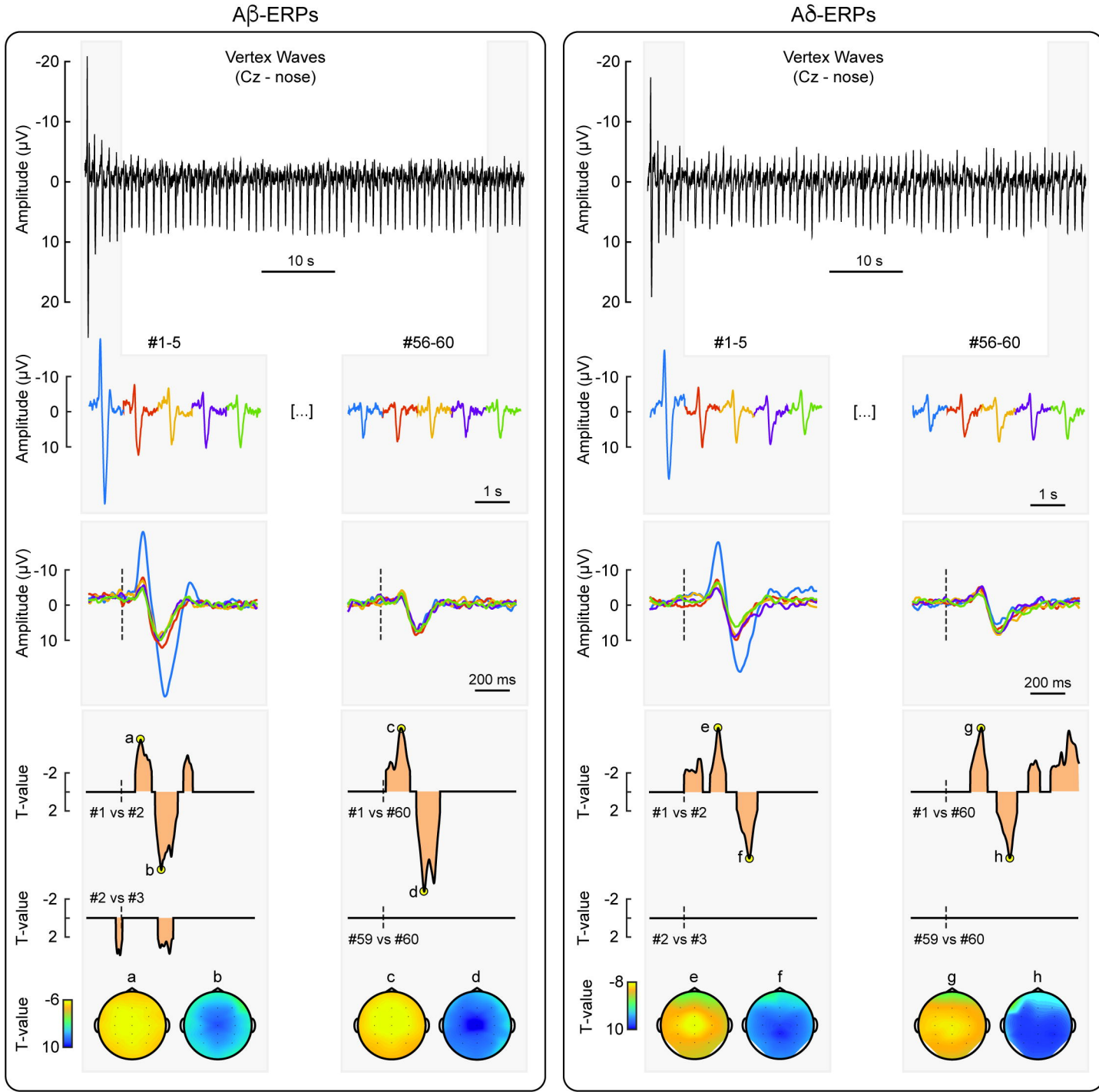
Aβ-ERPs
Aδ-ERPs
Vertex Waves
(Cz - nose)
Amplitude (μV)
-20
-10
0
10
20
10 s
#1-5
#56-60
[...]
1 s
200 ms
T-value
-2
2
#1 vs #2
#1 vs #60
#2 vs #3
#59 vs #60
-6
-8
a
b
c
d
e
f
g
h

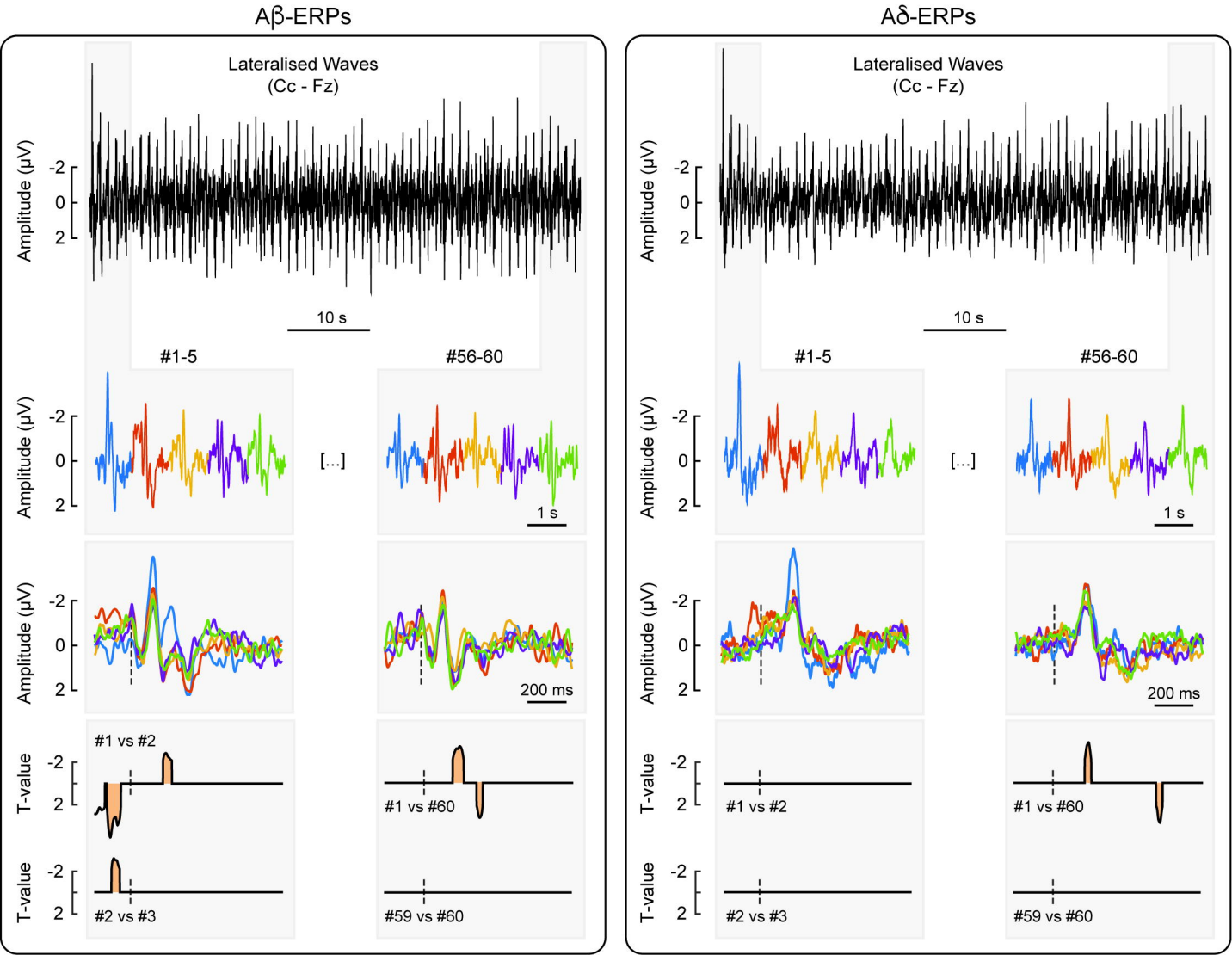
Aβ-ERPs
Aδ-ERPs
Lateralised Waves
(Cc - Fz)
Amplitude (µV)
-2
0
2
10 s
#1-5
#56-60
[...]
1 s
200 ms
T-value
#1 vs #2
#1 vs #60
#2 vs #3
#59 vs #60

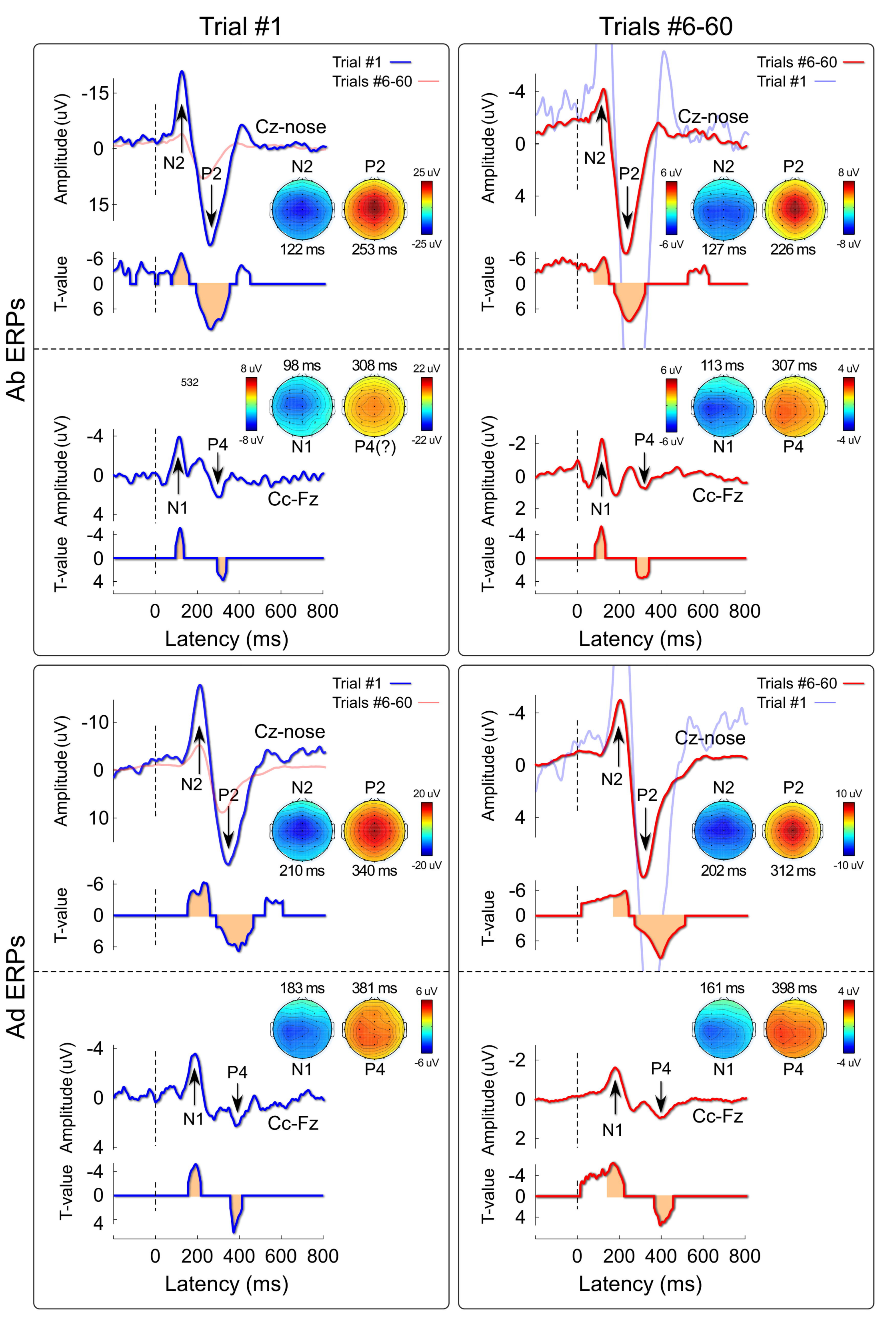
Trial #1
Trials #6-60
Ab ERPs
Ad ERPs
Trial #1
Trials #6-60
Cz-nose
N2
P2
122 ms
253 ms
25 uV
-25 uV
Amplitude (uV)
T-value
532
8 uV
-8 uV
98 ms
308 ms
22 uV
-22 uV
N1
P4(?)
P4
Cc-Fz
6 uV
-6 uV
113 ms
307 ms
4 uV
-4 uV
127 ms
226 ms
8 uV
-8 uV
210 ms
340 ms
20 uV
-20 uV
202 ms
312 ms
10 uV
-10 uV
183 ms
381 ms
6 uV
-6 uV
161 ms
398 ms
4 uV
-4 uV
Latency (ms)

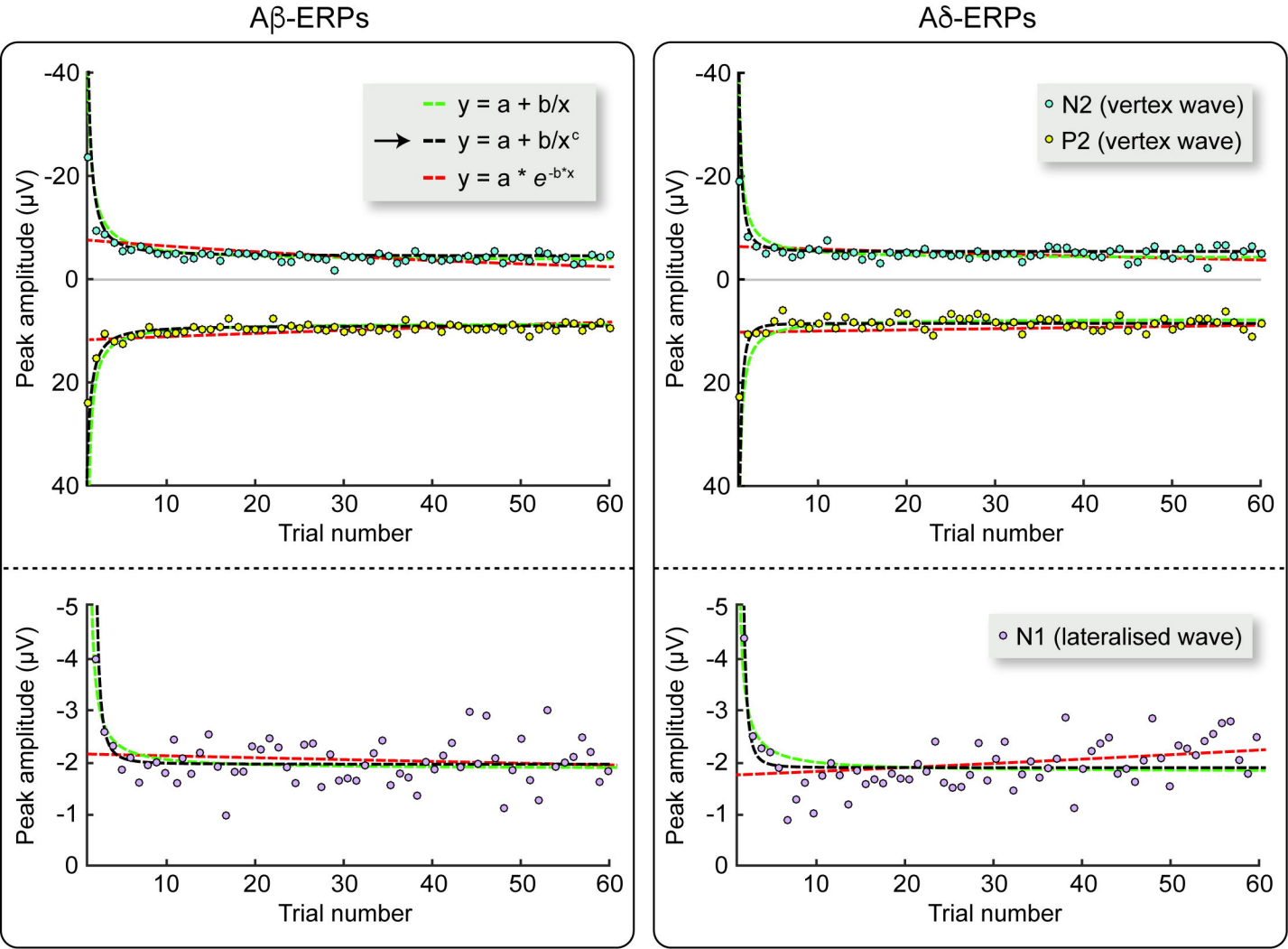
Aβ-ERPs
Aδ-ERPs
y = a + b/x
y = a + b/x^c
y = a * e^-b*x
N2 (vertex wave)
P2 (vertex wave)
N1 (lateralised wave)
Peak amplitude (μV)
Trial number
-40
-20
0
20
40
-5
-4
-3
-2
-1
0
10
20
30
40
50
60